inter-noise 88

A METHOD TO DETECT SEPARATELY SOUND INTENSITY OF TRAVELING WAVE IN EACH DIRECTION AT A POINT IN AIR-MOVING SYSTEM

Michihito TERAO and Hidehisa SEKINE

Faculty of engineering, Kanagawa University
Rokkaku-bashi 3-27-1, Kanagawa-ku,
Yokohama-shi, 221, JAPAN

A method to detect individual intensity vectors(i.i.v.'s) of approximated several plane waves arriving at a point has been studied. The i.i.v.'s are determined by solving a nonlinear equation system which relates unknown arriving wave pressures at a point to several adjacent sound pressures. Relations between the i.i.v.'s and net intensity vector (n.i.v.) are utilized to evaluate the error caused by finite number plane wave approximation. Numerical and laboratory tests have been carried out.

DETECTION OF INDIVIDUAL WAVE PRESSURES ARRIVING AT A POINT

Locating i-th sound pressure observation point sufficiently small distance $r_i=|\mathbf{r}_i|$ from the attractive point O as shown in Fig.1, the pressure P_i at i-th point $\mathbf{r}_i$ can be related to the contribution p_{ij} of j-th arriving plane wave whose pressure amplitude at point O is denoted by p_j as;

$$P_i=\sum_{j=1}^{N} p_{ij} = \sum_{j=1}^{N} p_j \exp(-jkr_i\cos\sigma_{ij}), \quad (i=1,M) \qquad (1)$$

where $k=2\pi\nu/c$ denotes wave number, ν frequency, c sound speed, and σ_{ij} the angle between $\mathbf{r}_i$ and unit direction vector $\mathbf{u}_j$ of j-th arriving wave, which can be expressed as;

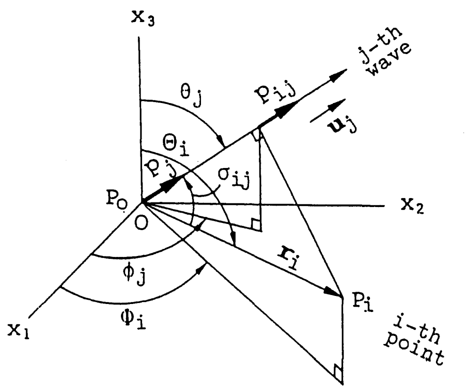

Fig.1 Relation between j-th arriving wave and sound pressure at i-th observation point

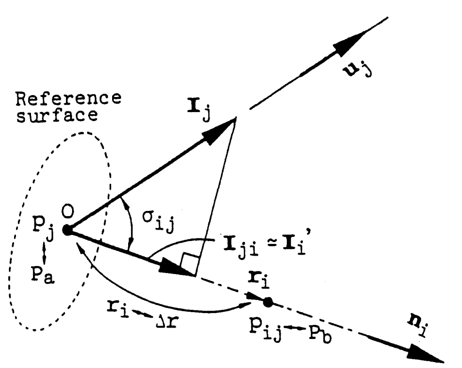

Fig.2 Relation between j-th i.i.v. and j-th pressure p_j

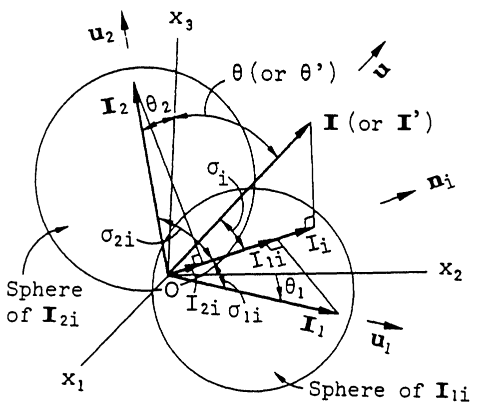

Fig.3 Vector sum $\mathbf{I}$(or $\mathbf{I}'$) of i.i.v.'s ($\mathbf{I}_j$'s)
In this case, $\mathbf{I}$(or $\mathbf{I}'$) $= \mathbf{I}_1 + \mathbf{I}_2$

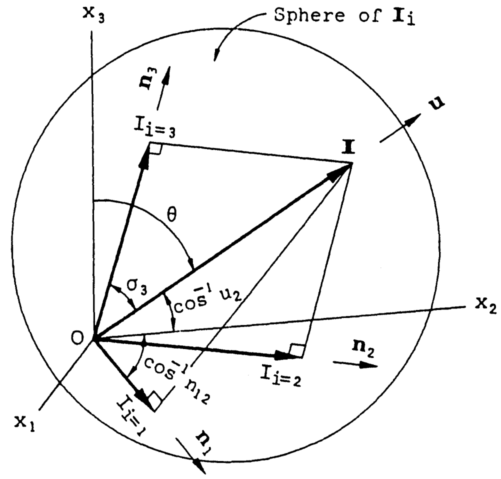

Fig.4 N.i.v. $\mathbf{I}$ and its $\mathbf{n}_i$ surface components ($\mathbf{I}_i$'s)

$$\cos\sigma_{ij} = \sin\Theta_i \sin\theta_j \cos(\Phi_i - \phi_j) + \cos\Theta_i \cos\theta_j \qquad (2)$$

N and M(=2N for 3D case) represent the total number of the arriving waves and observation points respectively. Making observation of P_i's, the nonlinear system of eqs.(1) can be solved numerically for each of the unknown p_j and $\mathbf{u}_j$(or θ_j and ϕ_j) of j-th arriving wave.

INDIVIDUAL ARRIVING WAVE INTENSITY VECTOR

The finite difference approxmation I_i' of the intensity I_i for a reference surface with normal unit vector $\mathbf{n}_i$ which is in the same direction from point a to b as shown in Fig.2 is, as well known, expressed as;

$$I' = -\mathrm{Im}(P_a^* P_b/2)/(\rho c k \Delta r) \qquad (3)$$

where P_a and P_b denote pressures at a and b, P_a^* the complex conjugate of P_a, Δr distance between the points, ρ density.

Defining I_{ji}' as the finite difference approximation of i-th arriving wave's intensity I_{ji} in $\mathbf{n}_i$ direction, and substituting I_{ji}' for I_i', p_j for P_a, p_{ij} for P_b, and r_i for Δr in the eq.(3) respectively, we obtaine

$$I_{ji} = \lim_{r_i \to 0} I_{ji}' = \lim_{r_i \to 0} \{-\mathrm{Im}(p_j^* p_{ij}/2)/(\rho c k r_i)\} = I_j \cos\sigma_{ij} = \mathbf{I}_j \cdot \mathbf{n}_i \qquad (4)$$

where, $\mathbf{I}_j$ is j-th i.i.v. and defined as;

$$\mathbf{I}_j = I_j \cdot \mathbf{u}_j \ , \text{ and } \ I_j = |p_j|^2/(2\rho c) \qquad (5)$$

NET INTENSITY VECTOR

Net intensity I_i in $\mathbf{n}_i$ direction for all the arriving waves can be, as shown in Fig.3, expressed as;

$$I_i = \sum_{j=1}^{N} I_{ji} = \sum_{j=1}^{N} (\mathbf{n}_i \cdot \mathbf{I}_j) = \mathbf{n}_i \cdot \left(\sum_{j=1}^{N} \mathbf{I}_j\right) = \mathbf{n}_i \cdot \mathbf{I}$$
$$= I\, \mathbf{u} \cdot \mathbf{n}_i = I \cos\sigma_i \qquad (6)$$

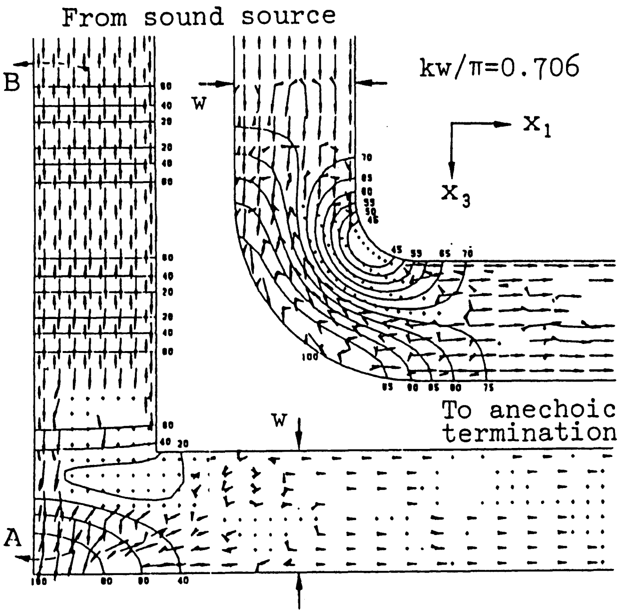

Fig.5 Distribution of major 2 i.i.v.'s for 2 types of elbows

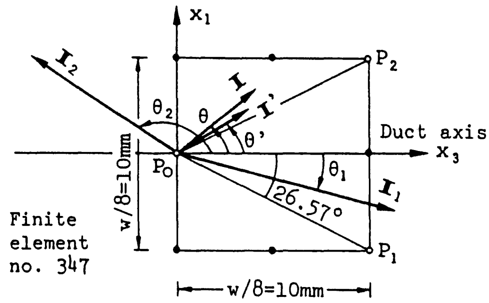

P_0=0.706+j×0.0159 I_1=0.0004643, θ_1=-14.17°
P_1=0.852+j×0.00000325 I_2=0.0005855, θ_2=145.67°
P_2=0.806+j×0.0292 I'=0.0002190, θ'=32.76°
I =0.0002720, θ =40.30°

a) Point A around discontinuity region

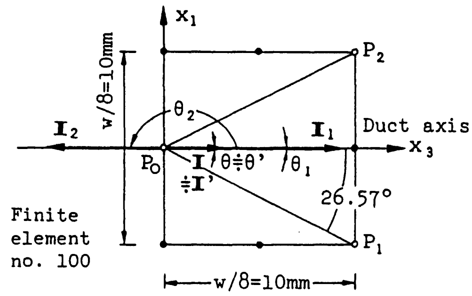

P_0=-0.722+j×0.249 I_1=0.0004541, θ_1=0.01°
P_1=-0.645+j×0.246 I_2=0.0003005, θ_2=180.01°
P_2=-0.645+j×0.246 I'=0.0001536, θ'=0.01023°
I =0.0001515, θ =-0.1015°

b) Point B in straight duct region

Fig.6 Details for the separated intensity vectors in Fig.5

where, $I=|\mathbf{I}|$, $\mathbf{u}=\mathbf{I}/I$, and σ_i represents the angle between $\mathbf{u}$ and $\mathbf{n}_i$, $\mathbf{I}(=I\mathbf{u})$ is the n.i.v. and defined by the vector sum of the i.i.v.'s, i.e.,

$$\mathbf{I}(\text{or } \mathbf{I}') = \sum_{j=1}^{N} \mathbf{I}_j \qquad (7)$$

Note that symbol $\mathbf{I}'$ will be used instead of $\mathbf{I}$, on the occasion of N taken smaller than total number of arriving waves.

Another well known method to determine n.i.v. is exists; making observation of net intensity I_i at every direction $\mathbf{n}_i=(n_{i1},n_{i2},n_{i3})$ for i=1,3 as shown in Fig.4 for 3D case, unknown $\mathbf{I}$ can be determined, independently of N, by solving the linear system of eqs.(6) or (8);

$$I_i = I\cos\sigma_i = I\sum_{\ell=1}^{3}(u_\ell n_{i\ell}) \text{ , and } \sum_{\ell=1}^{3} u_\ell^2 = 1 \qquad (8)$$

where u_ℓ and $n_{i\ell}$ denotes the direction cosines of unit vector $\mathbf{u}$ and $\mathbf{n}_i$ respectivly, with respect to the ℓ-th axis.

VALIDITY OF THE METHODS

Typical results by numerical tests are shown in Fig.5. Which illustrate two major acoustic energy flows $\mathbf{I}_1$ and $\mathbf{I}_2$ at every point around air duct elbows determined by using pressure distribution obtained by a finite element method as shown in Fig.5. $\mathbf{I}'$ the vector sum of $\mathbf{I}_1$ and $\mathbf{I}_2$, have been compared with $\mathbf{I}$ by $P_0^*P_1$, $P_0^*P_2$ and eq.(7). In Fig.5 the maximum

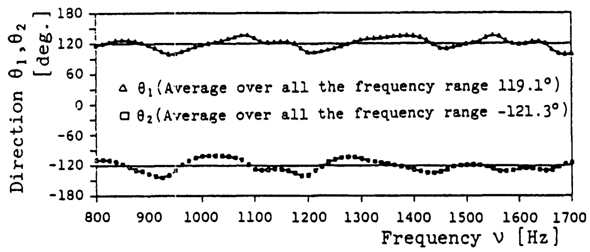

a) Detected directions

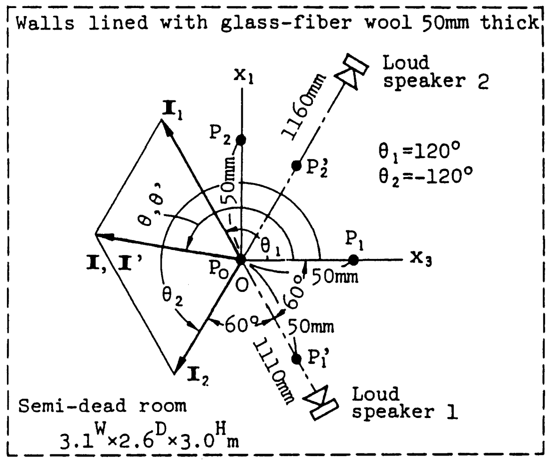

Fig.7 Arrangement of sound sources and observation points

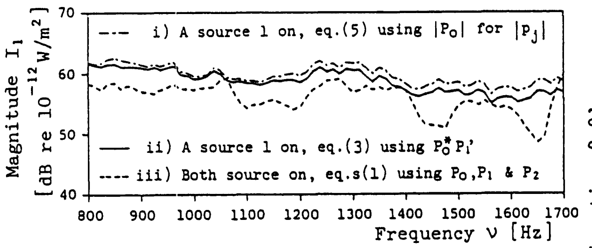

b) Magnitude of 1st major i.i.v. $\mathbf{I}_1$

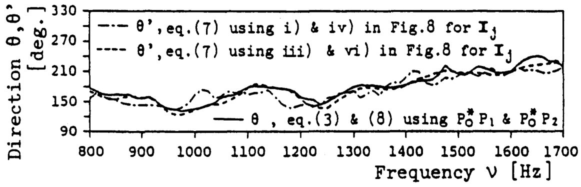

a) Direction

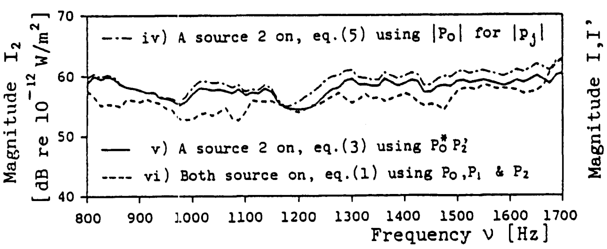

c) Magnitude of 2nd major i.i.v. $\mathbf{I}_2$

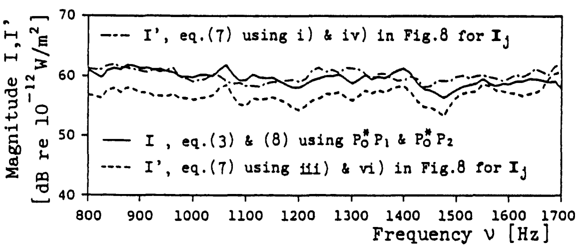

b) Magnitude

Fig.8 Separated major 2 i.i.v.'s $\mathbf{I}_1$ & $\mathbf{I}_2$

Fig.9 Determined n.i.v.'s $\mathbf{I}$ & $\mathbf{I}'$

error between these accepted, is 1/1.5 or 1.5 in magnitude and ±10° in direction: The symbol(·) shows the point with greater error than the above limit: The blank space is that of too small magnitude to illustrate. At point B, as might be expected, $\mathbf{I}_1$ and $\mathbf{I}_2$ are mutually in opposite and axial direction as well as $\mathbf{I}'$ coincident well with $\mathbf{I}$, which ensures the validity of the methods.

Laboratory tests to detect major two arriving waves $\mathbf{I}_1$ and $\mathbf{I}_2$ from two loud speakers at around ceteral point O in a small semi-dead room have been conducted as shown in Fig.7, Typical results are shown in Fig.8 and Fig.9, with those measured turning a speaker on and the other off. Although omission of free field correction of microphones as well as poor test set up, source direction identifications by i.i.v.'s are rather satisfactory, though the separated i.i.v.'s are relatively lower in magnitude.

SUMMARY

Methods to detect individual intensity vectors have been presented. Whose validity and effectivity have been confirmed fairly well with numerical experiments and satisfactory with laboratory tests.